Astron. Astrophys. 317, 637–645 (1997)

ASTRONOMY
AND
ASTROPHYSICS

HST polarization observations of the jet of M87⋆

A. Capetti[1], **F. D. Macchetto**[1,2], **W. B. Sparks**[1], **and J.A. Biretta**[1]

[1] Space Telescope Science Institute; 3700, San Martin Drive, Baltimore, MD 21218, USA
[2] Associated with the Astrophysics Division, Space Science Department of ESA; Estec, NL-2200 AG Noordwijk, The Netherlands

Received 13 September 1995 / Accepted 6 March 1996

Abstract. We present the results of pre-refurbishment HST polarization observations of the jet of M 87 taken with the Faint Object Camera in the ultraviolet and with the WF/PC-I in the visual. From these observations we produce polarization maps of unprecedentedly high resolution. The structure of the projected magnetic field is extremely complex and changes on the smallest observable scales. The degree of polarization increases from the center toward the edges of the jet where it reaches 60%. A comparison of these images with radio polarization maps shows no measurable depolarization or Faraday rotation.

The morphology of knot D is substantially different in the VLA observations by Owen et al. and these HST observations. The measured changes in knot D are inconsistent with proper motions and must be intrinsic to the jet structure. While the magnetic field configuration is remarkably similar at the locations of knots D2 and D3, the magnetic field appears to have changed from parallel to perpendicular at the location of knot D1. These results suggest that this component is associated with a shock front. Simultaneous polarization observations are required to determine if the changes in the magnetic structure are due to an intrinsic difference in the magnetic field configuration as seen by optical and radio emitting electrons or to a change of the jet structure, with the appearance of a new component.

Key words: galaxies: individual (M 87) – galaxies: jets – polarization

1. Introduction

Almost a century after the discovery of the first optical jet in the M 87 galaxy (NGC 4486, 3C 274 , Virgo A) by Curtis (1918) several hundreds extragalactic "jets" are known, almost all found at radio wavelengths (Bridle and Perley 1984). However, only a few of these have been detected in the optical region (e.g. Keel 1988). M 87, being the nearest to us, remains a prime target for multi-wavelengths studies of an extragalactic jet.

On the West side of the double lobed radio source, the radio jet extends $\sim 25''$ from the center of the galaxy. It shows a sequence of bright knots and relatively darker interknots regions (Owen et al. 1980). High resolution radio data (Owen et al. 1989) revealed that the emission on the knots has a filamentary structure suggesting that the emission is produced primarily in a boundary layer between the jet and the external medium. On the opposite SE side, even though no counter-jet has been detected, a ridge of radio emission, cospatial with a similar optical feature has been interpreted as due to the interaction of a jet with the external medium (Sparks et al. 1992; Stiavelli et al. 1992).

Proper motions of bright knots have been measured at radio wavelengths on both the parsec and kiloparsec scale resulting in the intriguing finding that the jet is sub-luminal on the pc scale (Reid et al. 1989) but some features on the kpc scale show apparent super-luminal motion (Biretta et al. 1995).

The optical and radio jet morphology appear to be similar on the large scale (e.g. Nieto and Lelièvre 1982). This apparent similarity was confirmed by early high resolution HST images (Boksenberg et al. 1992). However more detailed analysis has shown that significant and important differences (Sparks et al. 1995) exist in the appearance of the jet at different wavelengths. The optical emission is more concentrated than the radio emission and the optical jet is also narrower as also seen in 3C 273 (Thompson et al. 1993).

Prior to the 1993 refurbishment of HST, we obtained high resolution imaging polarimetry of the M 87 jet with HST. If the emission mechanism is synchrotron radiation, as is generally accepted, imaging polarimetry provides information on the direction and uniformity of the magnetic field. Compared to the radio observations, optical polarimetry explores the magnetic field structure in the locality of the highly energetic electrons emitting at these wavelengths. The temporal evolution of the emission and of the magnetic configuration can also be analyzed comparing these observations to previous high resolution radio measurements. Given the shorter lifetime, by several order of magnitude of the optically emitting electrons, it is reasonable to expect a much more more rapid response to changing condition

Send offprint requests to: A. Capetti

⋆ Based on observations with the NASA/ESA Hubble Space Telescope, obtained at the Space Telescope Science Institute, which is operated by AURA, Inc., under NASA contract NAS 5-26555.

Table 1. Log of observations

Instrument	Filters	ND filters	Exp. time
FOC	F320W+POL0	0	1500
FOC	F320W+POL0	1	1500
FOC	F320W+POL0	1	300
FOC	F320W+POL60	0	1500
FOC	F320W+POL60	1	1500
FOC	F320W+POL60	1	300
FOC	F320W+POL120	0	1500
FOC	F320W+POL120	1	1500
FOC	F320W+POL120	1	300

in the jet itself and a clearer, sharper measurement of structural changes.

This paper is structured as follows. Details of the observations and the data reduction process HST are given in Sect. 2; the results themselves are presented and discussed in Sect. 3 through 5. A summary is given in Sect. 6.

2. Observations and data reduction

M 87 was observed using the Faint Object Camera (FOC) and the Wide Field Planetary Camera (WF/PC-I) on board the *Hubble Space Telescope* as follows.

2.1. The FOC observations

Observations were taken in 1993 June 17 (before the Refurbishment Mission), in the f/96, 512 × 1024 mode (Paresce 1992); the pixel size was of $0\farcs022 \times 0\farcs022$ and the field of view about $11'' \times 22''$. Three different polarizer filters (POL0, POL60 and POL120) were used in combination with the wide ultraviolet filter F320W. Three exposures were obtained with each polarizer, with exposure times ranging from 300 to 1500 s with and without neutral density filters (see Table 1) to avoid saturation effects.

The data were processed to correct for geometric distortion using the grid of regularly spaced reseau marks on the faceplate of the detector; the data frames were then divided by normalized and geometrically corrected internal flat-field frames. The reseau marks were removed from the images with values taken from neighboring pixels. A flat-field linearity correction was applied on each image following the prescription by Jedrzejewski (1992).

The polarizers are known to produce a spatial displacement in the output images, with small but significant differences from filter to filter (Hodge 1995). The position of the nucleus and cross-correlation techniques were used to register the images.

The FOC count rate is limited by the pixel scan rate; on the nucleus and on knot A the images exceeded the maximum count rate and therefore are non linear or saturated. Furthermore, in the 512 × 1024 format the total counts per pixel are limited to the 8-bit maximum value of 255. To correct for these effects, we substituted saturated portions of the images with the appropriately scaled portions of the images taken with the neutral density filter F1ND. We chose a conservative count rate threshold of 0.5 counts s^{-1}. At this level we expect an instrumental non-linearity of $\sim 10\%$, however such a moderate non linearity is corrected by the Jedrzejewski (1992) algorithm so that the final uncertainty is no greater than 1%.

The contribution of the galaxy starlight was removed by fitting elliptical isophotes to corrected images and subtracting the model thus obtained.

All the images were deconvolved using Lucy's (1974) algorithm. Point Spread Functions have been built using the Tiny Tim software (Krist 1992) and the deconvolution was ended when the χ^2 has converged to $\sim 1\%$, which required 20 iterations.

The deconvolved and aligned images obtained with the three polarizers, I_0, I_{60} and I_{120}, were combined to produce maps of the Stokes parameters I, Q and U

$$I = \frac{2}{3}(I_0 + I_{60} + I_{120})$$

$$Q = \frac{2}{3}(2 \cdot I_0 - I_{60} - I_{120})$$

$$U = \frac{2}{\sqrt{3}}(I_{60} - I_{120})$$

and of polarized flux $I_P = (Q^2+U^2)^{1/2}$, percentage of polarization $P = \frac{I_P}{I}$ and position angle $\theta = 0.5\mathrm{arctg}(\frac{U}{Q})$. The data were "debiased" using the correction of Wardle & Kronberg (1974)

$$I_P = I_{P_{\rm obs}} \left(1 - \frac{\sigma_{I_P}}{I_{P_{\rm obs}}}\right)^{1/2}$$

where P and $P_{\rm obs}$ are the corrected and observed polarization flux and σ_P is the noise in the polarization image.

The statistical errors in the Stokes parameters were computed assuming Poisson noise in the images, and ignoring cross terms in the covariance matrix. The errors on the degree and position angle of the polarization are then estimated as

$$\sigma_P = \sqrt{2}N^{-1/2}$$

$$\sigma_\theta = \sqrt{2}N^{-1/2}P^{-1}$$

where N are the total counts.

Various effects can produce systematic errors in the FOC polarization measurements; including differences in the transmission curves of the polarizers and residual transmittance in the direction perpendicular to plane of polarization of the filter. Capetti et al. (1995) discussed the systematic errors of the HST/FOC polarization observations in detail and found that they amount to less than ~ 2 deg in the polarization position angle. The same careful reduction procedures were used in this work.

2.2. The WF/PC-I observations

WF/PC-I observations were taken in 1993, June 19, in the PC mode, with a pixel size of $0\farcs043 \times 0\farcs043$. The four 800 × 800

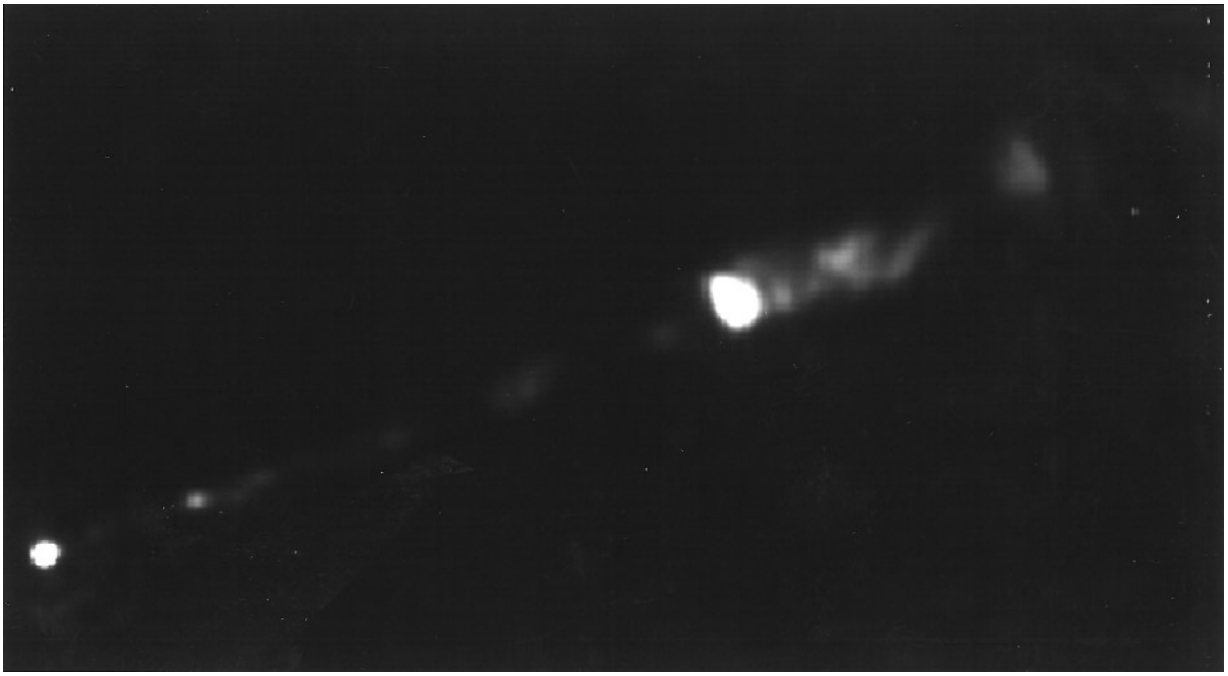

Fig. 1. Total intensity images of the M 87 jet in the near ultraviolet (F342W) from the FOC observations. The field of view is $9'' \times 5''$. North is at the top, East is to the left. All the images are presented in the same orientation

Fig. 2. Polarized flux images of the M 87 jet from the FOC observations. The field of view is $9'' \times 5''$. North is at the top, East is to the left

pixels CCD cover a field of view of $66'' \times 66''$. Three different polarizers were used in combination with the F555W filter and double exposures of 400 seconds were taken in each case. The data were processed by the WF/PC-I Science Data Processing pipeline which performs the following operations: bias level removal, bias image subtraction, preflash image scaling and subtraction, dark image scaling and subtraction and flat-field image correction (MacKenty et al. 1992).

Individual exposures were combined to remove cosmic rays. The resulting images were then deconvolved using 20 iterations of the Lucy's (1974) algorithm after subtraction of a smooth model of the diffuse galactic emission. The nucleus was used to register the images, and images were scaled according to the results of the HST WF/PC polarization calibration observations (see Capetti et al. 1995). Finally, the deconvolved and aligned images were combined to produce the polarization maps in the same way as for the FOC data.

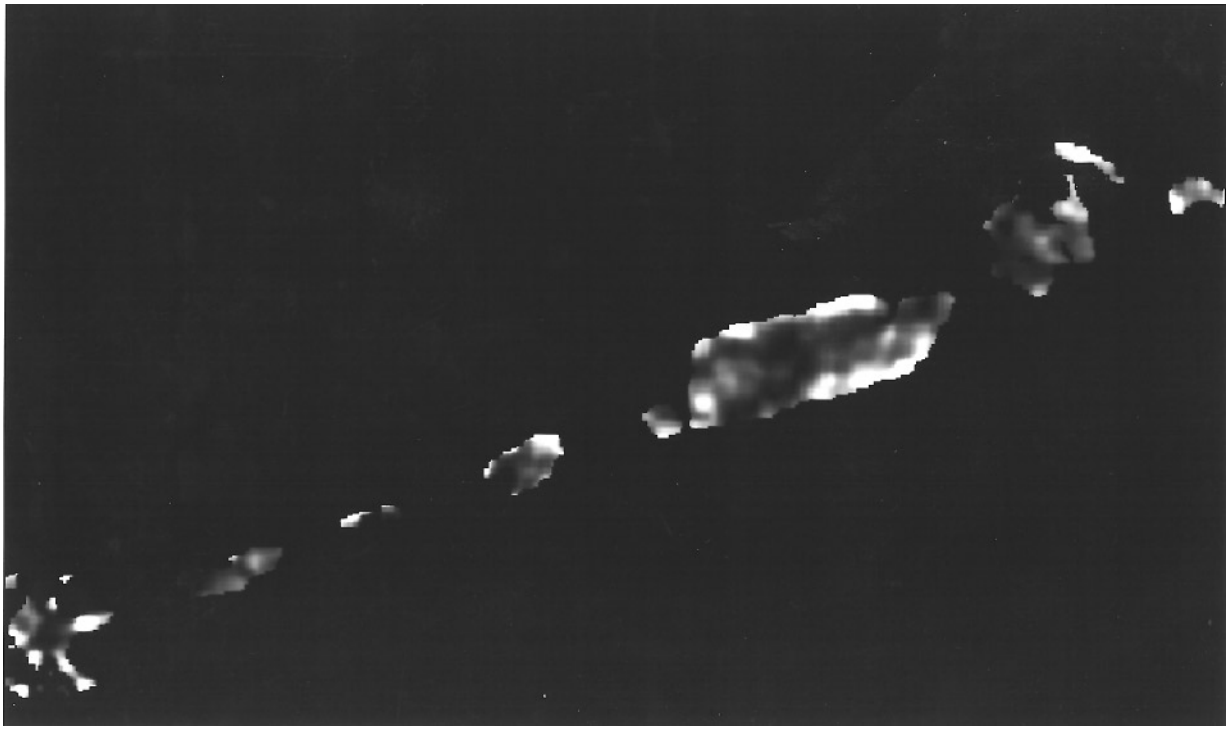

Fig. 3. Map of degree of polarization at 0.″2 resolution. Grey levels corresponds to percentage of polarization from 0% to 60% (form black to white). The field of view is $9'' \times 5''$

3. Polarization of the jet

Figure 1 shows the total intensity images obtained from the FOC observations. The HST resolution was degraded to 0.″2 FWHM by convolving with a Gaussian filter in order to obtain a good determination of the polarization parameters in the low surface brightness regions. The deconvolved images obtained with the two cameras are remarkably similar, providing circumstantial evidence vindicating the reliability of the deconvolution process. These images show very clearly the complex filamentary structure already known from the VLA (Owen et al. 1989) and HST observations (Boksenberg et al. 1992). We follow the standard nomenclature to refer to the emission knots along the jet, which are, at increasing distance from the nucleus, D, E, F, I, A (the brightest knot), B, C and G.

To compare our HST results with the 2 cm VLA images from Owen et al. (1989), we aligned the three sets of data by again using the position of the nucleus as a fiducial point. The accuracy in the consequent registration is estimated to be better than 0.″05, which is $\sim$ 1 pixel in the radio and WF/PC images. The optical synchrotron emission is less diffuse that the radio emission as discussed in detail by Sparks, Biretta & Macchetto (1995). Significant variations occurred in the jet between the VLA and HST observations at the location of knot D. These will be discussed in the next section. The differences between the optical and radio total intensity images are reflected in analogous differences in the polarized flux images, Fig. 2, which shows considerably less diffuse optical polarized emission along the edges of the jet when compared to the radio images.

Figure 3 shows the image of degree of polarization while Fig. 4 shows the pattern of the projected magnetic field from the both the FOC and the WF/PC-I observations at 0.″2 resolution.

On knot A and B, given their brightness, it is not necessary to degrade the resolution of the FOC images to estimate the polarization parameters and therefore full resolution polarization (0.″06) images can be produced for these regions (see Fig. 5).

The degree of polarization is typically 30% over most of the jet. Toward the edges of the jet the polarization increases, reaching values as high as 60%. In the regions of knot A and along the center of knot B the polarization appears to be lower, at around $\sim$ 10%. However, the full resolution images show that in these regions the magnetic field orientation changes on scales smaller than 0.″2 and therefore, due to the limited resolution of the images, local cancellation occurs reducing the observed value of the polarization.

The structure of the projected magnetic field is highly complex and varies on very small scales. On knot A, the magnetic field is perpendicular to the jet axis on the brightest regions but becomes parallel to the jet at its edges. At the onset of knot C the magnetic field structure appears to be circularly symmetric, and beyond this point the field parallels that of the jet filaments. On the first four knots it changes orientation from knot to knot and within one knot, being oblique or transverse at different locations.

The degree of polarization and the polarization pattern are overall very similar at radio and optical wavelengths (see Owen et al. 1989 for the radio observations). They may be compared quantitatively, and the results are "depolarization" images (the

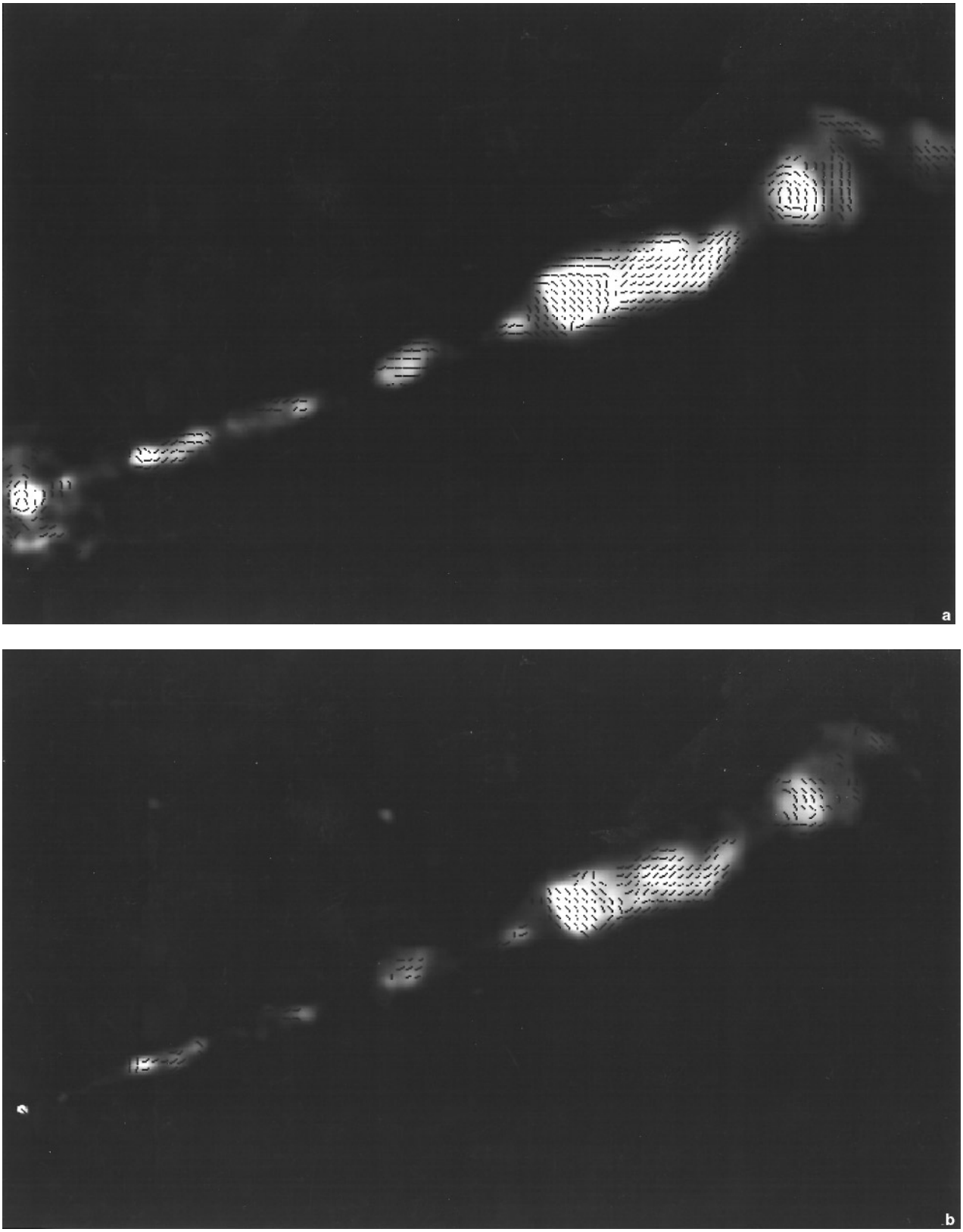

Fig. 4 a and b. Projected magnetic field configuration at $0.2''$ resolution superposed to the total intensity image for the a FOC and b WF/PC-I observations. To show more clearly the pattern, the length of the vectors is constant and not proportional to the polarization level. Vectors are drawn at $0.2''$ intervals

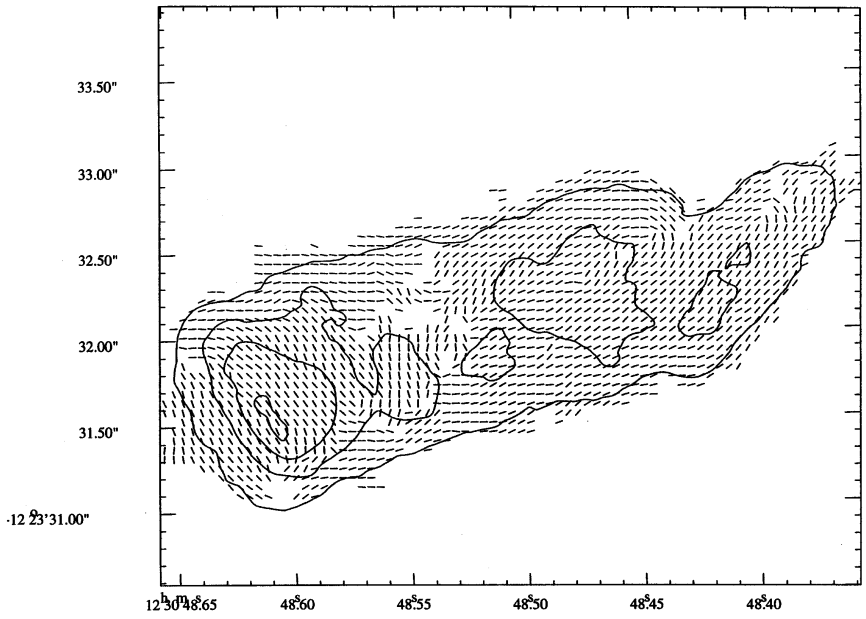

Fig. 5. Projected magnetic field configuration on knot A and B at $0.06''$ resolution. Superimposed are the total intensity contours

ratio between the VLA and HST degree of polarization) and of the difference of polarization position angles between the radio and optical (Fig. 6a and 6b).

The optical/radio difference in polarization angles are smaller than 20 degrees everywhere. This result is in accord with the determination of the rotation measure obtained from radio observations by Owen, Eilek & Keel (1990). They found $-350 < RM < 350$ rad m^{-2} over the whole length of the M 87 jet; if the rotation of the position angle follows a λ^2 law (Burns 1966), the expected difference between 2 cm and the UV will be less than 8 degrees. Over the whole jet the depolarization is less than 10%.

The non-linearity on knot A in the FOC images without neutral density filter can be as large as 15%. To check if the non-linearity has been removed adequately from the data, we estimated the polarization on this region. We found P = 33.5% and θ = 35° from the FOC, P = 32.8% and θ = 36° from the WF/PC-I and P = 31.0% and θ = 35° from the VLA. This shows that the FOC data are reliable in this region and that depolarization and rotation measure are negligible.

4. Proper motions and polarization changes

The morphology of knot D is substantially different in the VLA observations by Owen et al. and these HST observations. In particular, the distance between the first and the last component of this triple knot is $0.76''$ in the radio images and $1.12''$ as measured from the FOC images. In this region Biretta, Zhou & Owen (1995) measured proper motions corresponding to an apparent speed of up to 2.5 c. If the change between the radio and optical structure of knot D has to be attributed to proper motions, this would correspond to a relative speed of 11 c, inconsistent with that measured by Biretta, Zhou and Owen. Furthermore, comparing the HST images with VLA images taken in January 1993 (J. Biretta, private communication) similar differences are seen and they cannot be explained by proper motions on a time-scale as short as five months. This indicates that the optical and radio morphology of knot D are intrinsically different. Knot D1 appears to be relatively brighter and closer to the nucleus in the optical than in the radio images. Similarly, the optical emission from knot D3 arises at larger distances from the nucleus. This implies that the spectral index is flatter at the optical location of knot D1 and D3 than on the remaining of knot D.

In Fig. 7a and 7b we plot the projected magnetic field for this portion of the jet from the FOC and VLA observations at $0.2''$ resolution. The magnetic field configuration at the two epochs are remarkably similar at the locations of knots D2 and D3; in this region the average difference between the two datasets is only 2 degrees and the r.m.s. of this difference is also 2 degrees. However, it appears that knot D1 has evolved dramatically: in the HST image, the magnetic field swings from PA $\sim -60°$ to PA $\sim 0°$ at the peak of knot D1, while this change does not appear in the 1985 VLA image.

All the results obtained for knot D1 suggest that this is associated with a shock front. At the location of a shock front acceleration of relativistic electrons occurs (e.g. Bell 1978), enhancing the synchrotron emission at shorter wavelengths, and the transverse component of the magnetic field is amplified by the compression produced by the shock, in agreement with our observations.

Two alternative scenarios can explain the change in magnetic field observed at knot D1 between the VLA and the HST images. The optical synchrotron emission originates from a population of relativistic electrons with much higher energy than the radio synchrotron emission. Therefore they are possibly tracing different regions of the jet with different magnetic field configuration with respect to the bulk of radio emitting plasma. This is likely to be particularly relevant at the location of a shock front where acceleration of the higher energy electrons occurs. Alter-

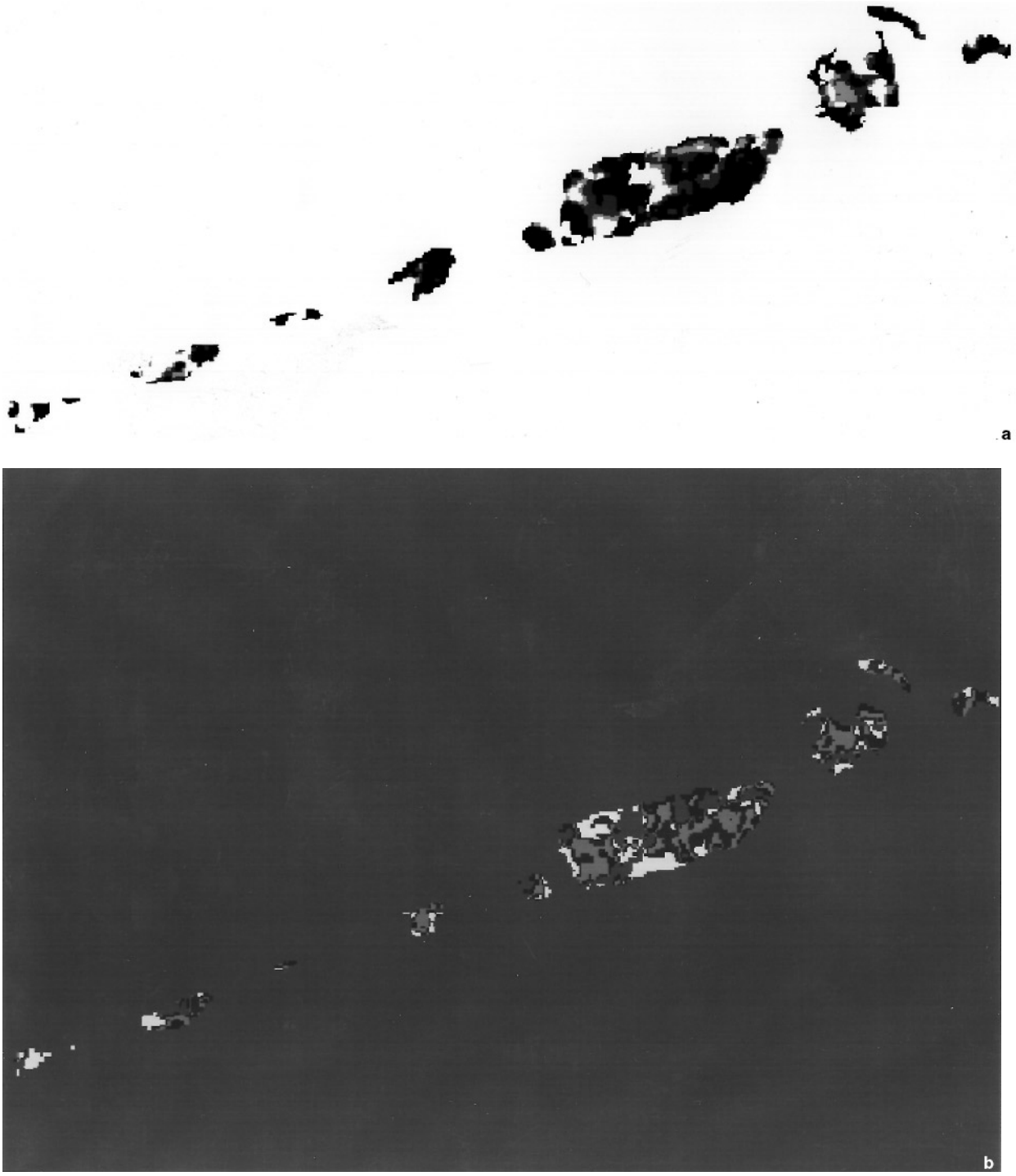

Fig. 6 a and b. Images of a rotation measure and b depolarization obtained comparing the VLA (Owen et al. 1989) and HST polarization images. Grey levels correspond to a difference in polarization angle of -20, -10, 0 and +10 degrees (from darker to lighter colors) and of a ratio of percentage of polarization measured in the radio versus the optical of 0.90 ,0.95 ,1.00 ,1.05 and 1.10 (again from darker to lighter colors)

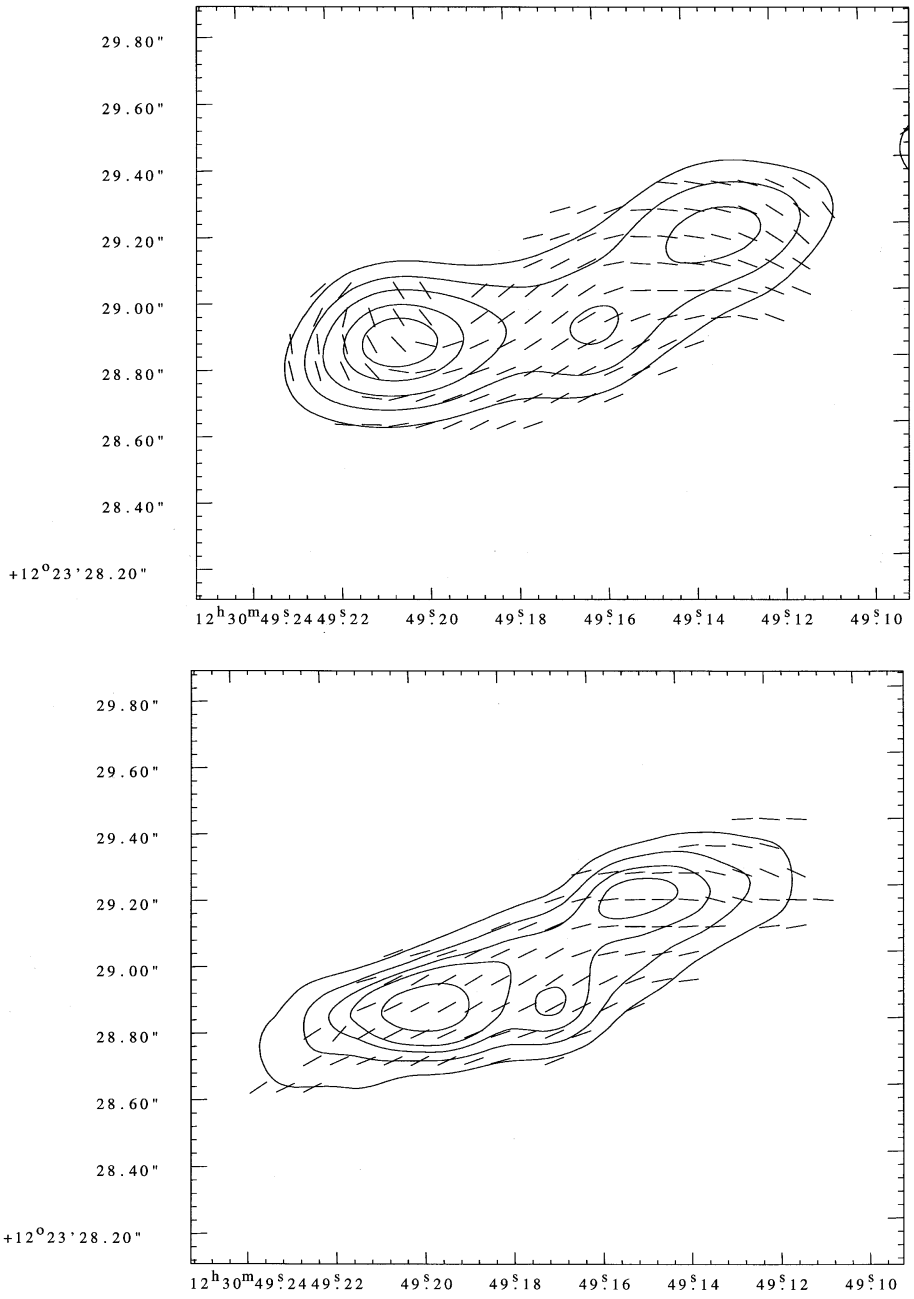

Fig. 7 a and b. Projected magnetic field configuration on knot D at $0.2''$ resolution from the (a) FOC and (b) VLA observations. Vectors are drawn at $0.1''$ intervals. Superimposed are the total intensity contours

natively, knot D1 is associated with a new component in the jet, which was not present at the time of the VLA observations.

Simultaneous radio and optical polarization images are required to distinguish between these alternatives.

5. Polarization of the nucleus

The unresolved nuclear source is marginally polarized in both the ultraviolet, $m = 2.9 \pm 0.5\%$ and $\theta = 12^\circ \pm 5^\circ$, and the visual $m = 1.6 \pm 0.7\%$ and $\theta = 45^\circ \pm 13^\circ$. These results are consistent with the $3\% \pm 2\%$ polarization level measured by Fraix-Burnet et al. (1989) in the U band.

At radio wavelengths the polarization of the nuclei of radiogalaxies is usually only a few percent (Jones et al. 1985) and they are significantly less polarized that the corresponding radio jets. This is also the case for M 87 (Owen et al. 1989). This effect can be explained as due to synchrotron self-absorption or cancellation produced by the superposition of several emitting components polarized at different position angles.

At optical wavelengths synchrotron self-absorption is negligible. On the other hand, significant dilution can be produced by non polarized optical emission, of stellar or nuclear origin. Furthermore, the polarization position angle measured on the nucleus is perpendicular, within the errors, to the radio-jet in both the visual and the ultraviolet. The observed polarization

can originate from the unresolved base of the jet if the magnetic field is, as observed over most of its length, preferentially aligned with the jet axis. From these data, we cannot distinguish between these three alternatives.

6. Summary and conclusions

We presented the results of pre-refurbishment HST polarization observations of the jet of M 87 taken with the FOC in the ultraviolet and with the WF/PC-I in the visual. From these observations we produce polarization maps of unprecedentedly high resolution. The degree of polarization is typically 30% over most of the jet. At the edges of the jet the polarization is as high as 60%, requiring a highly ordered magnetic field. In the center of the jet the small scale structure of the magnetic field produces significant cancellation reducing the polarization to $\sim 10\%$.

The structure of the projected magnetic field is very complex and varies on a small scales. On the first four knots it changes orientation from knot to knot and within one knot, being, oblique or transverse at different locations. At knot A, the magnetic field is perpendicular to the jet axis on the brightest regions and becomes parallel to the jet at its edges. At the onset of knot C the magnetic field structure appears to be circularly symmetric, beyond this point the field parallels that of the filaments.

The degree of polarization and the polarization pattern are very similar at radio and optical wavelengths. No significant depolarization or Faraday rotation have been detected, in agreement with previous radio determination.

The morphology of knot D is considerably different in the VLA observations by Owen et al. and these HST observations. The comparison with more recent VLA observations shows that this effect is not due to proper motions but can be explained if the spectral index on knot D1 and D3 is flatter than the rest of the D complex. While the magnetic field configuration is remarkably similar at the locations of knots D2 and D3, with an average difference of 2 degrees and a r.m.s. of 2 degrees, the magnetic field appears to have changed from parallel to perpendicular at the location of knot D1. This suggests that this component is associated with a shock front. At the location of a shock front acceleration of relativistic electrons occurs, enhancing the synchrotron emission at shorter wavelengths, and the transverse component of the magnetic field is amplified by the compression produced by the shock, in agreement with our observations. Simultaneous polarization observations are required to determine if the changes in the magnetic structure derived from radio and optical data are due to an intrinsic difference in the magnetic field configuration as seen by electrons of higher energy or if this is due to a change of the jet structure, with the appearance of a new component.

The unresolved nuclear source is marginally polarized in both the ultraviolet, $m = 2.9 \pm 0.5\%$ and $\theta = 12^\circ \pm 5^\circ$, and the visual $m = 1.6 \pm 0.7\%$ and $\theta = 45^\circ \pm 13^\circ$. From these data we cannot distinguish if the low degree of polarization is due to cancellation or dilution from unpolarized emission.

Acknowledgements. We would like to thank the referee, D. Fraix-Burnet, for his useful comments. AC acknowledges financial support from the StScI grant GO-4666 and GO-3594.

References

Biretta J.A., Zhou F., Owen F.N., 1995, ApJ 447, 582
Boksenberg A., et al., 1992, A&A 261, 393
Bridle A.H., Perley R.A., 1984, ARAA 22, 319
Burns J.O., 1986, ApJ 316, 175
Capetti A., Axon D.J., Macchetto F.D., Sparks W.B., Boksenberg A., 1995, ApJ 446, 155
Curtis H.D., 1918, Publ. Lick. Obs. 13, 9
Fraix-Burnet D., Le Borgne J.A., Nieto J.-L., 1989, A&A 224, 17
Hodge P., 1995, Faint Object Camera Science Report 89, Space Telescope Science Institute, Baltimore
Jedrzejewski R., 1992, Faint Object Camera Science Report 62, Space Telescope Science Institute, Baltimore
Keel W.C., 1988, ApJ 329, 532
Krist J., 1992, The Tiny Tim User's Manual, Space Telescope Science Institute, Baltimore
Lucy L.B., 1974, AJ 79, 745
MacKenty J.W., Griffiths R.E., Sparks W.B., Horne K., Gilmozzi R., Ewald S.P., Ritchie C.E., Baggett S.M., Walter L.E., Schneider G., 1992, Wide Field and Planetary Camera Instrument Handbook Version, Space Telescope Science Institute, Baltimore
Nieto J.-L., Lelièvre G., 1982, A&A 109, 95
Owen F.N., Hardee P.E., Cornwell T.J., 1989, ApJ 340, 698
Owen F.N., Eilek J.A., Keel W.C., 1990, ApJ 362, 449
Paresce F., 1992, Faint Object Camera Instrument Handbook Version, Space Telescope Science Institute, Baltimore
Reid M.J., Biretta J.A., Junor W., Muxlow T.W. B., Spencer R.E., 1989, ApJ 336, 112
Sparks W.B., Fraix-Burnett D., Macchetto F.D., Owen F.N., 1992, Nat 355, 804
Sparks W.B., Biretta J.A., Macchetto F.D., 1995, ApJ submitted
Stiavelli M., Biretta J., Moller P., Zeilinger W.W., 1992, Nat 355, 802
Thompson R.C., Mackay C.D., Wright A.E., 1993, Nat 365, 133
Wardle J.F.C., Kronberg P.P., 1974, ApJ 194, 249